Plastome of mycoheterotrophic *Burmannia itoana* Mak. (Burmanniaceae) exhibits extensive losses of photosynthesis genes along with unusual retention of genes and distinct rearrangements

Xiaojuan Li [1,2] , **Xin Qian** [1,2] , **Gang Yao** [3] , **Zhongtao Zhao** [Corresp., 1] , **Dianxiang Zhang** [Corresp. 1]

1 Key Laboratory of Plant Resources Conservation and Sustainable Utilization, South China Botanical Garden, Guangzhou, China

2 College of Life Sciences, University of Chinese Academy of Sciences, Beijing, China

3 South China Limestone Plants Research Center, South China Agricultural University, Guangzhou, China

Corresponding Authors: Zhongtao Zhao, Dianxiang Zhang
Email address: zhzht621@scbg.ac.cn, dx-zhang@scbg.ac.cn

The plastomes of heterotrophs went through varying degrees of degradation along with the transition from autotrophic to heterotrophic lifestyle. Here we examined the plastome of mycoheterotrophic species *Burmania itoana* and compared it with those of its reported relatives including three autotrophs and one heterotroph (*Thismia tentaculata*) in Dioscoreales. *B. itoana* yields a rampantly degraded plastome reduced in size and gene numbers at the advanced stages of degradation. Its length is 44,463 bp with a quadripartite structure, about thirty percent of the total length of the autotrophic relatives and nearly three times over that of *T. tentaculata*. The *B. itoana* plastome contains 39 unique genes (23 protein coding genes, 4 rRNAs and 12 tRNAs), with 33 putatively functional genes and six tentative pesudogenes. Among four inversions (Inv1/ Inv2/Inv3/Inv4) and four insertions (Ins1, Ins2, Ins3 and Ins4) detected in *B. itoana* plastome, Inv2 likely is consequence of the shift to heterotrophic lifestyle, and others may be associated with the mobile elements and recombination of distinct tRNA genes, respectively. Our results fill the gap of knowledge about the heterotroph plastomes in Burmanniaceae and provide a new evidence for the convergent degradation patterns of plastomes in plants en route to heterotrophic lifestyle.

1 **Plastome of mycoheterotrophic _Burmannia itoana_ Mak. (Burmanniaceae) exhibits**
2 **extensive losses of photosynthesis genes along with unusual retention of genes and distinct**
3 **rearrangements**

4 Xiaojuan Li[1, 2], Xin Qian[1, 2], Gang Yao[3], Zhongtao Zhao[*,1], Dianxiang Zhang[*,1]

5 [1] Key Laboratory of Plant Resources Conservation and Sustainable Utilization, South China
6 Botanical Garden, Chinese Academy of Sciences, Guangzhou 510650, China
7 [2] College of Life Sciences, University of Chinese Academy of Sciences, Beijing 100049, China
8 [3] South China Limestone Plants Research Center, College of Forestry and Landscape
9 Architecture, South China Agricultural University, Guangzhou 510642, China
10 [*]Corresponding authors: E-mails: zhzht621@scbg.ac.cn; dx-zhang@scbg.ac.cn

Introduction

Plastids were derived from a common cyanobacterial ancestor that established a permanent endosymbiotic relationship with mitochondriate ancestor (Gould et al. 2008; Ku et al. 2015). One nature of plastome is that its genes could be transferred or pruned. For instance, the ancestor genes of the plastid have transferred to other two genomes (nuclear and mitochondria) or lost during evolution (Martin and Herrmann 1998; Cusimano and Wicke 2016). Most plastomes of land plants are canonical circular and quadripartite including two inverted repeats (IRs) separated by larger single copy region (LSC) and small single copy region (SSC), and its lengths usually ranges from 120 kbp to 170 kbp with about 113 unique genes including about 79 protein-coding genes, 4 rRNA genes, and 30 tRNA genes (Wicke et al. 2011). These genes are classified into 3 main classes depending on functions: (1) photosynthesis related genes (ndh/atp/psa/psb/pet/ycf3/ycf4/rbcL); (2) transcription, transcript maturation and translation related genes (rpo/infA, matK and tRNAs/rRNAs/rps/rpl), (3) other non-bioenergetic function genes (accD/clpP/ycf1/ycf2/ccsA/cemA) (Bock 2007; Wicke et al. 2011).

Parasitic and mycoheterotrophic plants, which establish a physiological relationship with either plants or fungi to obtain organic and mineral nutrients, are referred to have partially or fully lost the capacity of photosynthesis (Wicke and Naumann 2018). The transition of lifestyle from autotrophic to heterotrophic may have left measurable clues in genomes, such as adaptive and non-adaptive changes (Wicke et al. 2016). Studies about plastomes of heterotrophs revealed that plastomes of heterotrophic plants experienced convergent degradation syndromes including overall decreases in genome size along with functional and physical gene losses, decrease in GC-content, increased frequency of rearrangements, accumulation of indels and losses of introns, *etc.*, compared with plastomes of autotrophs (Wicke et al. 2013; Logacheva et al. 2014; Lam et al. 2015; Lim et al. 2016; Wicke et al. 2016; Petersen et al. 2018; Schneider et al. 2018).

Hitherto, several conceptual models of plastome degradation have been proposed to account for the order of the heterotrophs plastomes degradation in a simplified and idealized manner. In general, plastome degradation follows five major stages (Barrett and Davis 2012; Barrett et al. 2014; Naumann et al. 2016; Wicke et al. 2016; Graham et al. 2017): (1) ndh genes become dispensable once plants have the ability of obtaining nutrients using heterotrophic way; (2) when the lifestyle transfer to obligate heterotrophic, most of photosynthesis related genes and some housekeeping genes are lost; (3) atp/rbcL and nonessential housekeeping genes are lost or functionally replaced; (4) other nonbioenergitic genes (e. g. accD, clpP, ycf1/2) are lost or functionally replaced; (5) all plastid genes are lost.

Burmania contains about 60 species spanning from autotrophic, hemi-mycoheterotrophic to mycoheterotrophic (Jonker 1938; Zhang 1999; Wu et al. 2010), providing an excellent model system for understanding the evolution of plastome responding to the lifestyle shift from autotrophic to heterotrophic. Although the plastome of autotrophic *Burmannia disticha* (Ma et al. 2018) has been described, the plastome of mycoheterotrophic species in *Burmannia* has never been reported, hindering our efforts in elucidation of plastid evolution in the genus. Aiming to provide new evidence in our understanding of the mechanism of plastid evolution in mycoheterotrophic angiosperms, here we focus on *Burmannia itoana*, a mycoheterotrophic perennial herb distributed in the coastal provinces of southern China and Ryukyu Islands of Japan (Jonker 1938; Zhang 1999; Wu et al. 2010). We sequenced the *B. itoana* plastome and examined its content and structure. We furthermore compared the plastome of *B. itoana* with those of its documented relatives (e. g. *B. disticha*, *T. tentaculata*) in Dioscoreales.

Materials and methods

52 **DNA extraction and sequencing**

53 Samples of *B. itoana* were collected from the Longmen Park, Guangdong Province, China. The voucher specimens
54 (LXJLM07) are deposited in the IBSC (Herbarium of South China Botanical Garden). Total DNA was extracted
55 using a DNeasy Plant Mini Kit (Qiagen, Hilden, Germany). The total DNA was used to generate libraries with
56 average insert size of 500 bp and sequenced using Illumina HiSeq 2000 with 150 bp paired-end read lengths.

57 **Plastome *de novo* assembly and annotation**

58 The plastome was assembled using CLC Genomics Workbench v9.0 (CLC BIO, Aarhus, Denmark) with parameters
59 as follows: wordsize 63, bubble size 50, minimal contig length 1000 bp. Three plastome-like contigs were picked
60 out through mapping all assembled contigs to the sequence of *B. disticha* plastome, and then these contigs were
61 merged using Geneious (version 11.1.5) (Kearse et al. 2012) to build draft plastomes. Specific primers were
62 designed to confirm the overlap of the aligned contigs and identify the borders of the LSC, SSC, and IRs regions
63 using through PCR and Sanger sequencing method. Validated complete plastome was annotated using GeSeq
64 (Tillich et al. 2017) with default sets. tRNAs were predicted using tRNAscan-SE (Schattner et al. 2005). Finally,
65 the plastome map was visualized using OGDRAW v. 1.2 (Lohse et al. 2007). The annotation of plastome is
66 summarized in Additional file 1.

67 **Data collection and Comparative analysis of plastomes**

68 Four reported plastomes of *B. itoana* relatives including *B. disticha* (Burmanniaceae), *T. tentaculata* (Thismiaceae),
69 *Tacca chantrieri* (Taccaceae), and *D. zingiberensis* (Dioscoreaceae) were downloaded from GenBank, and the
70 Genbank accession is MG792012, KX171421, KX171420 and NC_027090M, respectively.
71   The GC-content of plastome and the four junctions of LSC/IRB, LSC/IRA, SSC/IRB and SSC/IRA were
72 identified using Geneious version 11.1.5 (Kearse et al. 2012). Gene contents of plastomes were compared between
73 *B. itoana* and four reported species in Dioscoreales. Gene orders excluding copies in IRs were explored using
74 Mauve (Darling et al. 2004) plugged in Geneious.

75 # Results

76 **General characteristics of *B. itoana* plastome**

77 The *B. itoana* plastome represents a quadripartite circular molecule with 44,636 bp in length. It contains two larger
78 inverted repeat regions (IRA/IRB: 12,174 bp), separated by a large single-copy region (LSC: 18,441 bp) and a small
79 single-copy region (SSC: 1674 bp) (**Fig. 1**). The *B. itoana* plastome contains 39 genes (**Fig. 1**, **Fig. 2**). 33 genes are
80 putatively functional and 6 genes are putative pseudogenes. The presumably functional genes include 4 rRNA genes,
81 8 tRNA genes and 21 protein genes. The petG, rpl36, trnH_GUG, trnD_GUC, trnG_GCC and trmS_UGA are
82 putative pseudogenes. The rpl16, rpl2 and rps12 genes contains one intron (the 3-end intron of rps12 is absent),
83 respectively, and the clpP gene harbors two introns. The overall GC-content of *B. itoana* plastome is 32%, which is
84 lower than those of its autotrophic relatives but is higher than that of *T. tentaculata.* The GC-content of IR, LSC and
85 SSC in *B. itoana* is 37.8%, 24.5% and 32.4% (Table 1), respectively. The circular plastome was deposited in
86 GenBank under the Accession Number MK318822.

87 **Comparison of gene contents and order between Dioscoreales plastomes**

88   The plastomes of the *B. disticha*, *T. chantrieri* and *D. zingiberensis* contain 112 genes (**Fig. 2**). In *B. itoana* plastome,

89   rps16 is also lost, and the second intron of rps12 is lost while it is retained in autotrophs' plastomes. Like in *T.*

90   *tentaculata*, the *B. itoana* plastome is not just downsizing but also lost most photosynthesis related genes and some

91   housekeeping genes. However, in *B. itoana* plastome, one photosynthesis related genes, pseudogenized petG is

92   retained. *B. itoana* plastome shares the whole 12 genes retained in *T. tentaculata* plastome. In comparing with the *B.*

93   *itoana* plastome, degradation of *T. tentaculata* plastome goes further.

94   The alignment using Mauve showed the autotrophs' plastomes are general syntenic with the exceptions that the

95   inversion of the SSC in *B. disticha*, and extremely modified plastome of *T. tentaculata* (**Fig. 3**). Here, we mainly

96   focus on the comparison between the plastome structure of the *B. itoana* and *B. disticha* represented in **Fig. 1** and

97   **Fig. 3**. The results showed that the gene order of *B. itoana* plastome exhibits eight rearrangements including four

98   inversions (Inv1, Inv2, Inv3, Inv4) and four insertions (Ins1, Ins2, Ins3 and Ins4) versus the *B. disticha* plastome.

99   Inv1 contains the cluster of trnS_GUA - trnG_GCC - trnfM_CAU - rps14 (ca. 1282 bp), and Inv2 just contains accD

100 (ca. 2725 bp), and both are located in LSC. Inv3 contains the cluster of rps7 - rps12 - rrn16 -rrn23 - rrn4.5 - rrn5 (ca.

101 6678 bp) stretching across the IRs and SSC, and Inv4 contains the cluster of rrn16 - rrn23 - rrn4.5 - rrn5 (ca. 5007

102 bp) located in IRs. Ins1 and Ins2 contain the cluster of partial truncate ndhD - rpl32 (ca. 720 bp), and both Ins3 and

103 Ins4 contain rps15 - truncate ycf1 - trnN (ca. 1900 bp). The cluster in Ins1/Ins2 is located in the SSC of all

104 autotrophic plastomes, and the cluster in Ins3/Ins4 is located in IRs and SSC of *B. disticha* plastomes and IRs of *T.*

105 *chantrieri* plastomes.

106 **Boundaries of SC/IRs of Dioscoreales plastomes**

107 The boundary of LSC/IR in *B. itoana* plastome slightly expands to rps3, which is different from that in its

108 autotrophic relatives. For example, the boundary of LSC/IR *B. disticha* is located in rpl22, and those of *T. chantrieri*

109 and *D. zingiberensis* are located in the intergenic space of rps19 and trnH_GUG. The boundaries of SSC/IR in *B.*

110 *itoana* plastome reside in rps7. In contrasting to that, the boundaries of SSC/IR are located in the intergenic of rps15

111 and ycf1, the ycf1 in *B. disticha* and *D. zingiberensis*, respectively. In *T. chantrieri*, one boundary of SSC/IR is

112 expanded to the intron of ndhA plastome. In summary, the IRs are expanded in both plastomes of *B. itoana* and *B.*

113 *disticha* relative to others. The boundaries of SC/IRs of Dioscoreales plastomes are showed in **Fig. 1**.

114 **Discussion**

115 **Convergent evolution of plastomes in heterotrophs**

116 Accompanying with forfeiting of photosynthetic capabilities, the plastomes of heterotrophic plants undergo

117 varying degrees of degradation of size and gene contents (Wicke et al. 2013; Wicke et al. 2016). For instance, the

118 largest is that of heterotrophic chlamydomonadalean alga *Polytoma uvella* with about 230 kb in length (Figueroa-

119 Martinez et al. 2017) , while the smallest sequenced plastome is 11, 348 bp in endoparasitic *Pilostyles aethiopica*

120 (Bellot and Renner 2015). Moreover, other studies reported that plastome has been possibly lost in green algal

121 genus *Polytomella* (Smith and Lee 2014) and land flowering plant *Rafflesia lagascae* (Molina et al. 2014). Our

122 results showed that *B. itoana* plastome displays a typical quadripartite architecture with LSC and SSC separated by

123 IRs consistent with that of canonical land plant plastomes. The length of *B. itoana* platome is only one-third of its

124 autotrophic relative *B. disticha* and is nearly three times that of *T. tentaculata*. As previously mentioned, gene losses

125 in plastomes of heterotrophs follow five stages (Barrett and Davis 2012; Barrett et al. 2014; Naumann et al. 2016;

126   Graham et al. 2017; Wicke and Naumann 2018). Our results showed that the *B. itoana* plastome is likely at the
127   fourth stage with nonbioenergitic and housekeeping genes (e. g. ycf1/2, rps23/tRNAs) being physically or
128   functionally lost. Losses of ycf1 and ycf2 in *B. itoana* plastome support that a general core set of genes (ycf1, ycf2,
129   accD, clpP, infA and trnE) varies among heterotrophs (Bellot and Renner 2015; Schelkunov et al. 2015; Lim et al.
130   2016; Naumann et al. 2016; Roquet et al. 2016).

131   It is a well-accepted tenet that matK encodes one kind of protein required for group IIA intron splicing of
132   seven plastid genes trnV_UAC, trnI_GAU, trnK_UUU, trnA_UGC, rpl2, rps12 (3-end intron) and atpF (Liere and
133   Link 1995; Zoschke et al. 2010). Normally, the group IIA intron will not be spliced out from the transcripts
134   without matK. Parallel losses of matK and group IIA intron-containing genes have occurred in *Cuscuta* (McNeal et
135   al. 2009). In *B. itoana* plastome, matK is physically lost accompanying with the loss of other 6 genes, however, the
136   rpl2 and rps12 are retained. Similarly, in the plastomes of *Cynomorium coccineum*, *Rhizanthella gardneri* and
137   *Epipogium aphyllum*, the absence of matK or truncated matK is also along with rps12 lost the second intron and
138   intact rpl2 (Delannoy et al. 2011; Bellot and Renner 2015; Schelkunov et al. 2015). The introns of both rpl2 and
139   rps12 are still sustained while the matK are absent in *Hydnora visseri* plastome, and all rps12 and rpl2 are
140   transcribed properly, however, both the rps12 and rpl2 appear to be pseudogenes in *Hydnora longicollis* (Naumann
141   et al. 2016). A large proportion of the matK genes in some species of orchids are pseudogenes while all seven genes
142   with group II introns are retained (Kim et al. 2014; Feng et al. 2016). These instances of matK loss or
143   pseudogenization with retention of group IIA introns may be because that the function of matK are recovered by that
144   of genes from nucleus (Mohr and Lambowitz 2003), or some group IIA introns may be able to self-splice (Kim et
145   al. 2014).

146   Like others at the advanced stage of degradation, the *B. itoana* plastome lost most of plastid encoded tRNAs
147   and only holds 12 tRNAs (eight functional and four pseudogenized). Two tRNAs (trnE_UUC and trnfM_CAU) are
148   shared within most heterotrophs. It was a plausible explanation that the two tRNAs are essential for haem
149   biosynthesis and mitochondrial protein synthesis, respectively, and cannot be replaced with their cytosolic
150   orthologues (Barbrook et al. 2006). However, the subset of tRNAs remained in *B. itoana* plastome has not been
151   detected in others. For instance, it shares only eight tRNAs with *R. gardneri* (containing 10 tRNAs) (Delannoy et al.
152   2011), seven with *E. roseum* (containing eight tRNAs) (Schelkunov et al. 2015) and six with *Sciaphila densiflora*
153   (containing six tRNAs) (Lam et al. 2015). Moreover, only two were found in *T. tentaculata* (Merckx et al. 2017)
154   and *Sciaphila thaidanica* (Petersen et al. 2018), and no functional tRNAs was found in two endoparasitic species of
155   *Pilostyles* (Bellot and Renner 2015). These suggest that the tRNAs loss is likely unique and undergoes varying
156   degrees within heterotrophs.

157   **Unusual retention of genes in *B. itoana* plastome**

158   Generally, plastomes of heterotrophs which at the fourth stage of degradation begin to shed all coding regions for
159   photosynthetic pathway (Barrett et al. 2014; Graham et al. 2017; Wicke and Naumann 2018). Attractively, the
160   frame of petG, which encodes a subunit protein of the cytochrome b6/f complex for the connection of PSI and PSII
161   (Bock 2007; Wicke et al. 2011), is idiosyncratically retained in *B. itoana* plastome but is not detected in other
162   heterotrophs at the advanced stage of degradation. In *B. itoana*, petG is proximate to trnW_CCA and accD. However,
163   the petG is lost while trnW_CCA and accD are intact in the plastomes of *R. gardneri* and *S. densiflora* (Delannoy et
164   al. 2011; Lam et al. 2015). Otherwise, functional loss of petG indicates that it is nonessential in *B. itoana* plastome.
165   Therefore, it could not been explained using the proposal that proximity to the essential gene or essential function

166 can help genes escaping from being lost (Lohan and Wolfe 1998). One study suggested that holding pseudogenes
167 illustrates that the plastome is undergoing the further degradation (Naumann et al. 2016).

168   In heterotrophs, the ribosomal genes begin to be absent from plastomes with varying degrees at the advanced
169 stages (Barrett and Davis 2012; Barrett et al. 2014; Naumann et al. 2016; Wicke et al. 2016; Graham et al.
170 2017). So far, no study reported functional or physical loss of rpl36 while rpl32, rpl20, rpl22, rpl23 and rpl33 are
171 retained. Interestingly, rpl36 become a pseudogene in *B. itoana*. Some factors, such as short length, location in
172 conserved operon or difficulty to be replaced by plastid compartments, may contribute to the retention of genes
173 (Lohan and Wolfe 1998; Wicke et al. 2013; Wicke et al. 2016). Commonly, rpl36 is located in the intergenic
174 space of rps11 and infA in the most conservative operon including almost all of ribosomal protein-coding genes.
175 Therefore, residing in essential operon and adjacent essential genes could not prevent rpl36 from being
176 pseudogenized in *B. itoana* plastome. It's plausible to speculate that the function of rpl36 is not essential, or its loss
177 can be compensated by other intracellular genomes in *B. itoana* plastome (Schelkunov et al. 2015; Cusimano and
178 Wicke 2016; Naumann et al. 2016; Petersen et al. 2018).

179   Among the ribosomal genes, rps15 and rpl32 are the first batch of genes to be absent from the reported
180 plastomes at the advanced stage of degradation. However, the rps15 and rpl32 are still retained and putatively
181 functional in *B. itoana* plastome. Previous study suggested that there is a strong positive correlation between the
182 number of putatively functional genes and plastome length among heterotrophic angiosperms (Barrett and Kennedy
183 2018). To date, the two genes rps15 and rpl32 are only preserved in reported plastomes whose length are longer than
184 80 kb only except the *Monotropa hypopitys* plastome with ca. 40 kbp in length (Ravin et al. 2016). In *B. itoana*
185 plastome, rps15 and rpl32 are resided in IRs, typically located in SSC. Previous studies proved that two copies of
186 genes in IR offer more opportunities to correct the aberrant mutations (Zhu et al. 2016; Choi et al. 2018). Thus, we
187 could reasonably speculate that IRs may shelter these genes from being deleted in *B. itoana* plastome.

188 **Different origination of rearrangements in *B. itoana* plastome**

189 It has been showed that some rearrangements are correlated with intermolecular recombination between distinct
190 tRNA (Hiratsuka et al. 1989; Haberle et al. 2008; Barrett and Kennedy 2018). In typical autotrophs' plastomes,
191 the cluster in Inv1 is part of the cluster of trnS_UGA – psbZ -trnG_GCC-trnfM_CAU - rps14 - psaB - psaA - ycf3 -
192 trnS_GGA in *B. disticha* plastome. We postulate that the recombination of trnS_UGA and trnS_GGA may resulted
193 in the Inv1 of *B. itoana* plastome. The Inv2 containing accD is also present in the plastomes of heterotrophic plants
194 *Petrosavia stellaris* and *S. densiflora* (Logacheva et al. 2014; Lam et al. 2015). This inversion is in a block mainly
195 consisting of the photosynthesis related genes, most of which were lost in *B. itoana* plastome. Thus, it is a plausible
196 explanation that gene losses may trigger the inversion along with the shift from autotroph to heterotroph. Few
197 rearrangements are located in the middle IR in land plants plastomes with exceptions in plastomes of some ferns,
198 Geraniaceae and Campanulaceae (Knox 2014; Weng et al. 2014; Robison et al. 2018). It was hypothesized that
199 MORFFO (mobile open reading frames) elements are regularly associated with inversions and changes to the
200 inverted repeats (Robison et al. 2018). Interestingly, the six rearrangements (Inv3/Inv4/Ins1/Ins2/Ins3/ins4) occur
201 in IRs-SSC, IRs, IRs and IRs of *B. itoana* plastome, respectively. The patterns of these rearrangements are
202 analogous to those of rearrangements in several plastomes of ferns (Robison et al. 2018). Therefore, we suppose
203 that these insertions may be MORFFOs in the *B. itoana* plastome.

204 **Conclusion**

205 Consistent with convergent evolution of plants plastomes en route to heterotroph, *B. itoana* plastome exhibits
206 rampant degradation and distinct rearrangements. Based on models of plastome evolution, the *B. itoana* plastome is
207 at the advanced stages of degradation, and the occurrence of six putative pseudogenes suggests that it could undergo
208 further degradation. Unusual retention of genes indicates that complex constraints affect the fate of the plastomes in
209 heterotrophs. Although, heterotrophs share a universal pattern of plastome degradation, each species holds a unique
210 plastome, accurately. In general, our study fills the gap of knowledge about the plastome of heterotrophs in
211 Burmanniaceae, and it would be attractive to investigate dense intraspecific or interspecific plastomes to
212 characterize the trajectories of plastomes evolution.

Acknowledgments

214 This study was supported by the National Natural Science Foundation of China (Grants 31600185 and
215 U1603231), and Ministry of Science and Technology of China (Grant 2013FY111200).

216 **Conflict of Interest:** The authors declare that they have no conflict of interest.

References

218 Barbrook AC, Howe CJ, Purton S (2006) Why are plastid genomes retained in non-photosynthetic organisms?
219   Trends Plant Sci 11:101-108 doi:10.1016/j.tplants.2005.12.004
220 Barrett CF, Davis JI (2012) The plastid genome of the mycoheterotrophic *Corallorhiza striata* (Orchidaceae) is in
221   the relatively early stages of degradation. American journal of botany 99:1513-1523 doi:10.3732/ajb.1200256
222 Barrett CF, Freudenstein JV, Li J, Mayfield-Jones DR, Perez L, Pires JC, Santos C (2014) Investigating the path of
223   plastid genome degradation in an early-transitional clade of heterotrophic orchids, and implications for
224   heterotrophic angiosperms. Mol Biol Evol 31:3095-3112 doi:10.1093/molbev/msu252
225 Barrett CF, Kennedy AH (2018) Plastid genome degradation in the endangered, mycoheterotrophic, north American
226   orchid *Hexalectris warnockii.* Genome Biol Evol 10:1657-1662 doi:10.1093/gbe/evy107
227 Bellot S, Renner SS (2015) The plastomes of two species in the endoparasite genus *Pilostyles* (Apodanthaceae) each
228   retain just five or six possibly functional genes. Genome biology and evolution 8:189-201
229   doi:10.1093/gbe/evv251
230 Bock R (2007) Structure, function, and inheritance of plastid genomes. In: Bock R (ed) Cell and Molecular Biology
231   of Plastids, vol 19. Topics in Current Genetics. Springer, pp 29-63. doi:10.1007/4735_2007_0223
232 Choi KS, Jeong KS, Ha Y-H, Choi K (2018) Complete chloroplast genome sequences of *Clematis* IR expansion and
233   relative rates of synonymous substitutions. doi:10.20944/preprints201804. 0106.v1
234 Cusimano N, Wicke S (2016) Massive intracellular gene transfer during plastid genome reduction in nongreen
235   Orobanchaceae. New Phytologist 210:680-693 doi:10.1111/nph.13784
236 Darling ACE, Mau B, Blattner FR, Perna NT (2004) Mauve: Multiple alignment of conserved genomic sequence
237   with rearrangements. Genome Res 14:1394-1403 doi:10.1101/gr.2289704
238 Delannoy E, Fujii S, Colas des Francs-Small C, Brundrett M, Small I (2011) Rampant gene loss in the underground
239   orchid *Rhizanthella gardneri* highlights evolutionary constraints on plastid genomes. Mol Biol Evol 28:2077-
240   2086 doi:10.1093/molbev/msr028
241 Feng YL et al. (2016) Lineage-Specific reductions of plastid genomes in an orchid tribe with partially and fully

242   mycoheterotrophic species. Genome biology and evolution 8:2164-2175 doi:10.1093/gbe/evw144

243   Figueroa-Martinez F, Nedelcu AM, Smith DR, Reyes-Prieto A (2017) The plastid genome of *Polytoma uvella* is the

244   largest known among colorless algae and plants and reflects contrasting evolutionary paths to

245   nonphotosynthetic lifestyles. Plant physiology 173:932-943 doi:10.1104/pp.16.01628

246   Gould SB, Waller RF, McFadden GI (2008) Plastid evolution. Annual review of plant biology 59:491-517 doi:

247   10.1146/annurev.arplant.59.032607.092915

248   Graham SW, Lam VK, Merckx VS (2017) Plastomes on the edge: the evolutionary breakdown of mycoheterotroph

249   plastid genomes. The New phytologist 214:48-55 doi:10.1111/nph.14398

250   Haberle RC, Fourcade HM, Boore JL, Jansen RK (2008) Extensive rearrangements in the chloroplast genome of

251   *Trachelium caeruleum* are associated with repeats and tRNA genes. J Mol Evol 66:350-361

252   doi:10.1007/s00239-008-9086-4

253   Hiratsuka J et al. (1989) The complete sequence of the rice (*Oryza sativa*) chloroplast genome: Intermolecular

254   recombination between distinct tRNA genes accounts for a major plastid DNA inversion during the evolution

255   of the cereals. Molecular General Genetics 217:185-194 doi:10.1007/bf02464880

256   Jonker FP (1938) A monograph of the Burmanniaceae. Kemink en zoon,

257   Kearse M et al. (2012) Geneious Basic: An integrated and extendable desktop software platform for the organization

258   and analysis of sequence data. Bioinformatics 28:1647

259   Kim JS, Kim HT, Kim J-H (2014) The largest plastid genome of monocots: a novel genome type containing AT

260   residue repeats in the slipper orchid *Cypripedium japonicum*. Plant Molecular Biology Reporter 33:1210-1220

261   doi:10.1007/s11105-014-0833-y

262   Knox EB (2014) The dynamic history of plastid genomes in the Campanulaceae sensu lato is unique among

263   angiosperms. Proc Natl Acad Sci U S A 111:11097-11102 doi:10.1073/pnas.1403363111

264   Ku C, Nelson-Sathi S, Roettger M, Garg S, Hazkani-Covo E, Martin WF (2015) Endosymbiotic gene transfer from

265   prokaryotic pangenomes: Inherited chimerism in eukaryotes. Proc Natl Acad Sci U S A 112:10139-10146

266   doi:10.1073/pnas.1421385112

267   Lam VK, Soto Gomez M, Graham SW (2015) The highly reduced plastome of mycoheterotrophic *Sciaphila*

268   (Triuridaceae) is colinear with its green relatives and is under strong purifying selection. Genome biology and

269   evolution 7:2220-2236 doi:10.1093/gbe/evv134

270   Liere K, Link G (1995) RNA-binding activity of the matK protein encodecd by the chloroplast trnk intron from

271   mustard (*Sinapis alba* L.). Nucleic Acids Res 23:917-921

272   Lim GS, Barrett CF, Pang CC, Davis JI (2016) Drastic reduction of plastome size in the mycoheterotrophic *Thismia*

273   *tentaculata* relative to that of its autotrophic relative *Tacca chantrieri*. American journal of botany 103:1129-

274   1137 doi:10.3732/ajb.1600042

275   Logacheva MD, Schelkunov MI, Nuraliev MS, Samigullin TH, Penin AA (2014) The plastid genome of

276   mycoheterotrophic monocot *Petrosavia stellaris* exhibits both gene losses and multiple rearrangements.

277   Genome biology and evolution 6:238-246 doi:10.1093/gbe/evu001

278   Lohan AJ, Wolfe KH (1998) A subset of conserved tRNA genes in plastid DNA of nongreen plants. Genetics

279   150:425-433

280   Lohse M, Drechsel O, Bock R (2007) OrganellarGenomeDRAW (OGDRAW): a tool for the easy generation of

281   high-quality custom graphical maps of plastid and mitochondrial genomes. Curr Genet 52:267-274

282   Ma L, Ma P, Li D (2018) The first complete plastid genome of *Burmannia disticha* L. from the mycoheterotrophic

283   monocot family Burmanniaceae. Plant Diversity 40:232-237 doi:10.1016/j.pld.2018.07.004

284   Martin W, Herrmann RG (1998) Gene transfer from organelles to the nucleus: How much, what happens, and why?

285   Plant physiology 118:9-17 doi:10.1104/pp.118.1.9

286   McNeal JR, Kuehl JV, Boore JL, Leebens-Mack J, dePamphilis CW (2009) Parallel loss of plastid introns and their

287   maturase in the genus *Cuscuta.* PLoS One 4:e5982 doi:10.1371/journal.pone.0005982

288   Merckx VSFT et al. (2017) The biogeographical history of the interaction between mycoheterotrophic *Thismia*

289   (Thismiaceae) plants and mycorrhizal *Rhizophagus* (Glomeraceae) fungi. J Biogeogr 44:1869-1879

290   doi:10.1111/jbi.12994

291   Mohr G, Lambowitz AM (2003) Putative proteins related to group II intron reverse transcriptase/maturases are

292   encoded by nuclear genes in higher plants. Nucleic Acids Res 31:647-652 doi:10.1093/nar/gkg153

293   Molina J et al. (2014) Possible loss of the chloroplast genome in the parasitic flowering plant *Rafflesia lagascae*

294   (Rafflesiaceae). Mol Biol Evol 31:793-803 doi:10.1093/molbev/msu051

295   Naumann J et al. (2016) Detecting and characterizing the highly divergent plastid genome of the nonphotosynthetic

296   parasitic plant *Hydnora visseri* (Hydnoraceae). Genome biology and evolution 8:345-363

297   doi:10.1093/gbe/evv256

298   Petersen G, Zervas A, Pedersen HAE, Seberg O (2018) Genome Reports: Contracted genes and dwarfed plastome in

299   Mycoheterotrophic *Sciaphila thaidanica* (Triuridaceae, Pandanales). Genome biology and evolution 10:976-

300   981 doi:10.1093/gbe/evy064

301   Robison TA, Grusz AL, Wolf PG, Mower JP, Fauskee BD, Sosa K, Schuettpelz E (2018) Mobile elements shape

302   plastome evolution in ferns. Genome biology and evolution 10:2558-2571 doi:10.1093/gbe/evy189

303   Roquet C et al. (2016) Understanding the evolution of holoparasitic plants: the complete plastid genome of the

304   holoparasite *Cytinus hypocistis* (Cytinaceae). Annals of botany 118:885-896 doi:10.1093/aob/mcw135

305   Schattner P, Brooks AN, Lowe TM (2005) The tRNAscan-SE, snoscan and snoGPS web servers for the detection of

306   tRNAs and snoRNAs. Nucleic Acids Research 33: W686

307   Schelkunov MI, Shtratnikova VY, Nuraliev MS, Selosse MA, Penin AA, Logacheva MD (2015) Exploring the

308   limits for reduction of plastid genomes: a case study of the mycoheterotrophic orchids *Epipogium aphyllum*

309   and *Epipogium roseum.* Genome biology and evolution 7:1179-1191 doi:10.1093/gbe/evv019

310   Schneider AC, Braukmann T, Banerjee A, Stefanovic S (2018) Convergent plastome evolution and gene loss in

311   holoparasitic Lennoaceae (Boraginales). Genome biology and evolution doi:10.1093/gbe/evy190

312   Smith DR, Lee RW (2014) A Plastid without a Genome: Evidence from the Nonphotosynthetic Green Algal Genus

313   *Polytomella.* Plant physiology 164:1812-1819 doi:10.1104/pp.113.233718

314   Tillich M, Lehwark P, Pellizzer T, Ulbricht-Jones ES, Fischer A, Bock R, Greiner S (2017) GeSeq - versatile and

315   accurate annotation of organelle genomes. Nucleic Acids Res 45

316   Weng ML, Blazier JC, Govindu M, Jansen RK (2014) Reconstruction of the ancestral plastid genome in

317   Geraniaceae reveals a correlation between genome rearrangements, repeats, and nucleotide substitution rates.

318   Mol Biol Evol 31:645-659 doi:10.1093/molbev/mst257

319   Wicke S et al. (2013) Mechanisms of functional and physical genome reduction in photosynthetic and

320   nonphotosynthetic parasitic plants of the broomrape family. Plant Cell 25:3711-3725

321   doi:10.1105/tpc.113.113373

322   Wicke S, Muller KF, dePamphilis CW, Quandt D, Bellot S, Schneeweiss GM (2016) Mechanistic model of

323   evolutionary rate variation en route to a nonphotosynthetic lifestyle in plants. Proc Natl Acad Sci U S A

324   113:9045-9050 doi:10.1073/pnas.1607576113

325   Wicke S, Naumann J (2018) Molecular evolution of plastid genomes in parasitic flowering plants. In: Chaw S-M,

326   Jansen RK (eds) Advances in Botanical Research, vol 85. Academic Press, pp 315-347. doi:

327   https://doi.org/10.1016/bs.abr.2017.11.014

328   Wicke S, Schneeweiss GM, dePamphilis CW, Muller KF, Quandt D (2011) The evolution of the plastid

329   chromosome in land plants: gene content, gene order, gene function. Plant molecular biology 76:273-297

330   doi:10.1007/s11103-011-9762-4

331   Wu D, Zhang D, Saunders. RMK (2010) Burmanniaceae Wu, ZY, Raven, PH and Hong, DY (Eds), Flora of China

332   23:121-125

333   Zhang D (1999) Systematics of *Burmannia* L. (Burmanniaceae) in the old world Hku Theses Online

334   Zhu A, Guo W, Gupta S, Fan W, Mower JP (2016) Evolutionary dynamics of the plastid inverted repeat: the effects

335   of expansion, contraction, and loss on substitution rates. The New phytologist 209:1747-1756

336   doi:10.1111/nph.13743

337   Zoschke R, Nakamura M, Liere K, Sugiura M, Boerner T, Schmitz-Linneweber C (2010) An organellar maturase

338   associates with multiple group II introns. Proc Natl Acad Sci U S A 107:3245-3250

339   doi:10.1073/pnas.0909400107

340

Fig. 1 Plastome structure of five species in Dioscoreales.

All genes are colored according to functional complexes. Genes shown left the line are transcribed counterclockwise, those right the line are transcribed clockwise. The light red blocks show inversions and light blue blocks show insertions. Genes containing intron(s) are marked with the symbol *. Pseudogenes and truncated genes are marked with "&" and "#", respectively. The inverted repeats (IRs) are shown with bold lines.
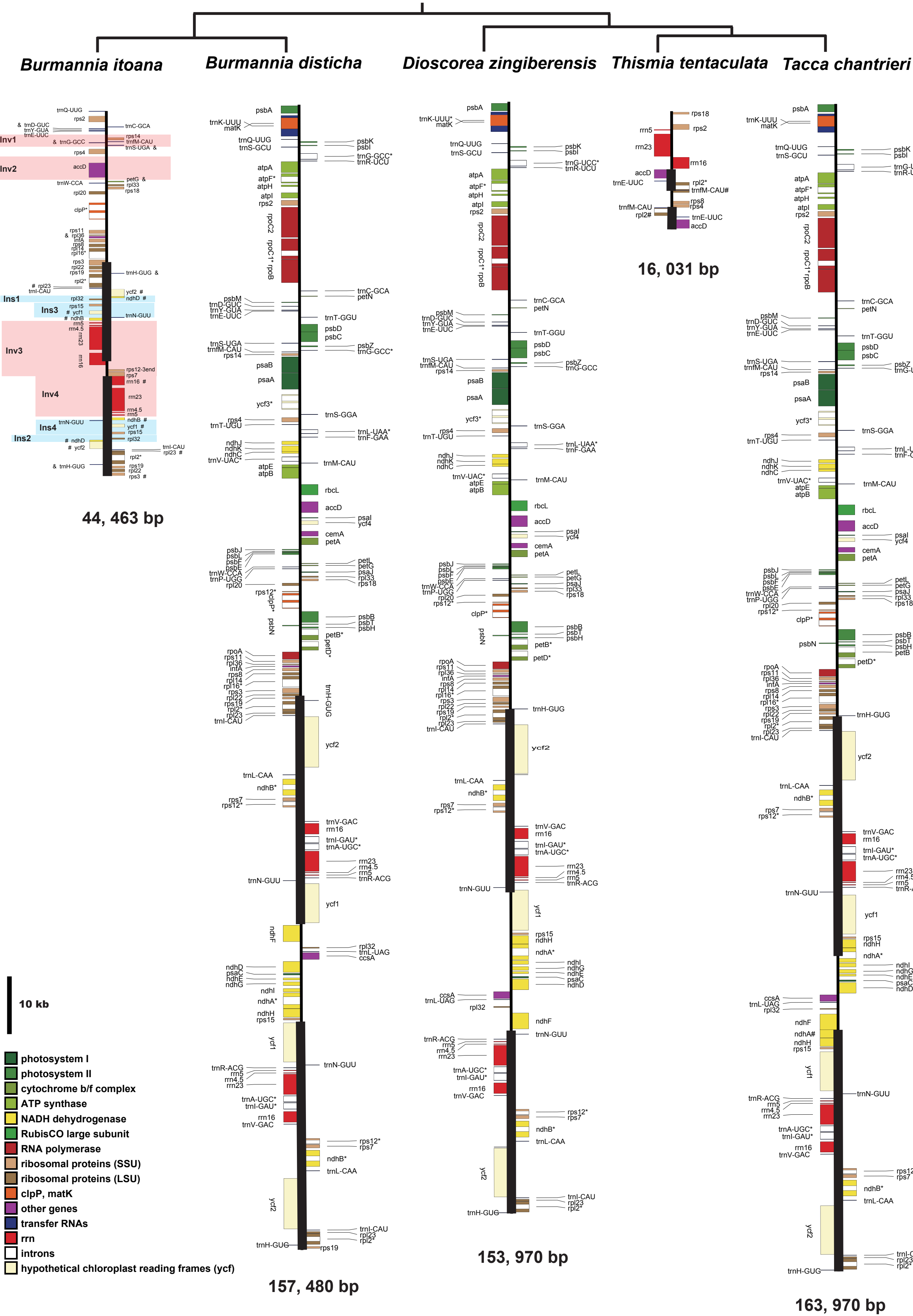
Fig. 2 Heat map showing gene contents in five species in Dioscoreales.

Genes in blue are retained and presumed fully functional; those in red are absent and those in yellow are putative pseudogenes. Gene names of photosynthesis related genes, genetic apparatus genes and other genes are in green, black, and red, respectively.
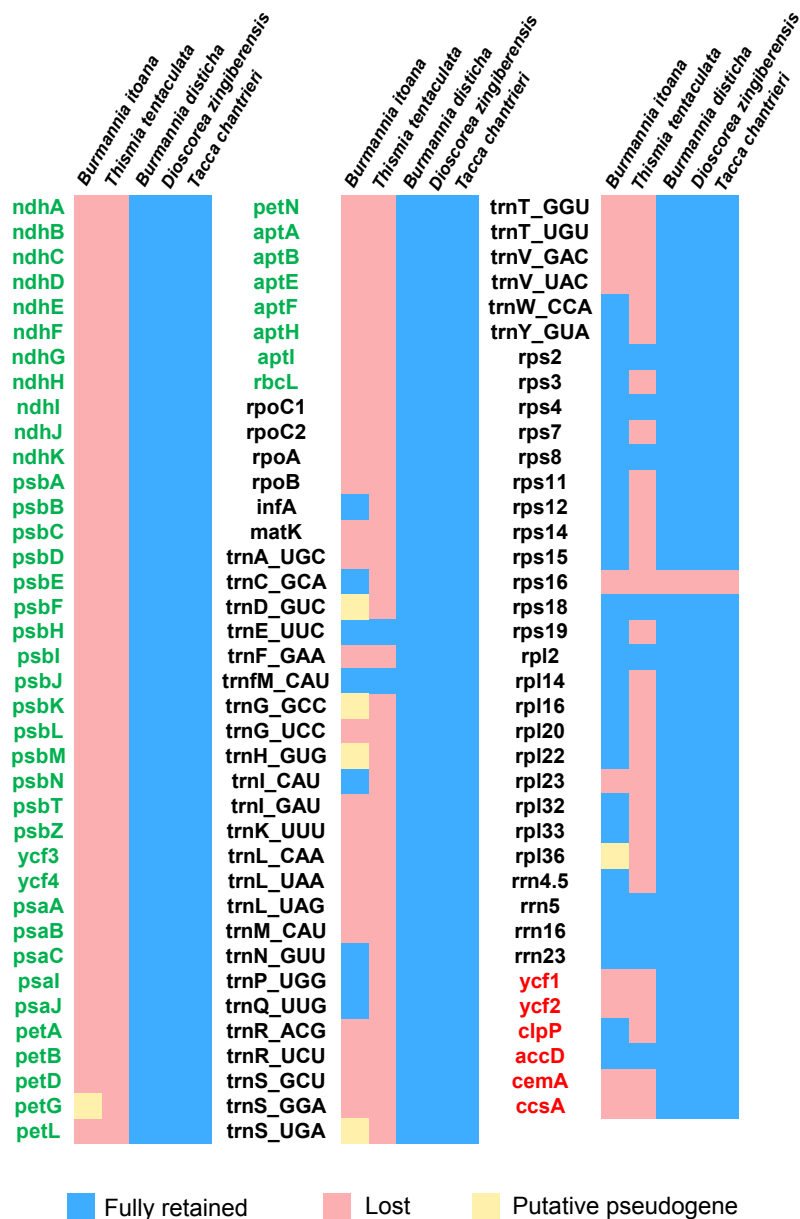
Fig. 3 Synteny of plastomes from five species .

The dashed lines and olidlines illustrate rearranged gene blocks and collinear between the two plastomes, respectively.
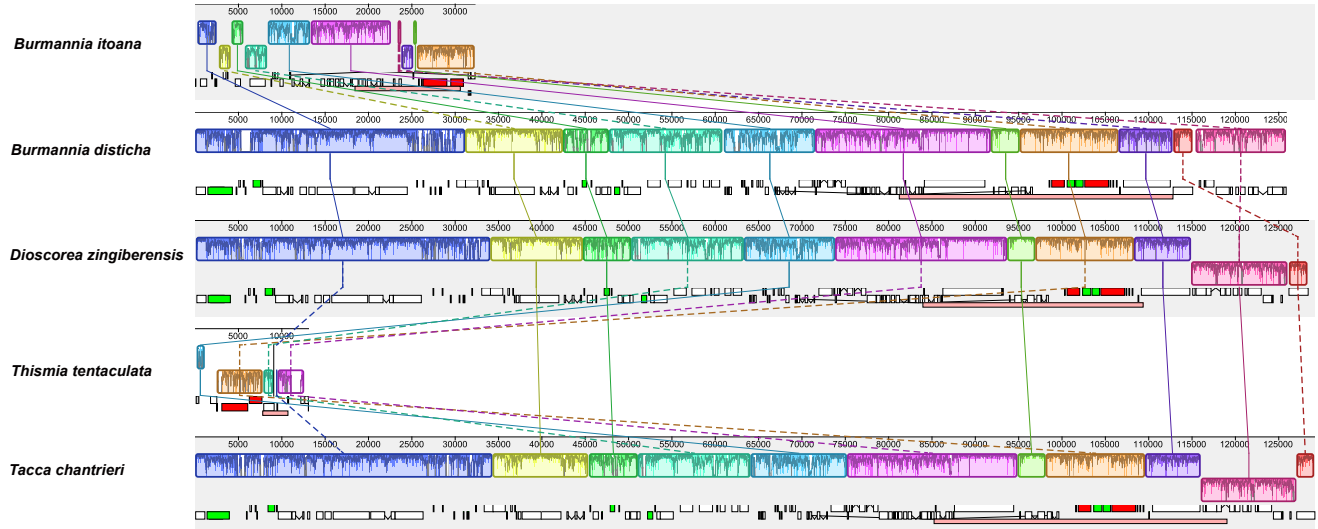
Table 1. General information of plastomes from five species in Dioscoreales.

Taxon	Length (bp) /GC-content (%)				Gene number		
	Total	IR	LSC	SSC	rRNAs	tRNAs	Protein coding
Burmannia itoana	44463/32.0	12174/37.8	18441/24.5	1674/32.3	4	12	23
Burmannia disticha	157480/34.9	31616/39.5	81231/32.3	13017/28.8	4	30	78
Dioscorea zingiberensis	153970/37.2	25491/43.0	83950/35.1	19038/31.2	4	30	78
Tacca chantrieri	163007/36.7	33837/40.3	85241/34.7	10092/30.6	4	30	78
Thismia tentaculata	16031/27.2	2948/30.0	7799/29.1	2336/13.7	3	2	7